

Research Article

Ian H. Williams*

Virtual transition states

<https://doi.org/10.1515/pac-2025-0453>

Received March 4, 2025; accepted May 6, 2025

Abstract: Many organic reaction mechanisms are complex and may involve both multiple steps in series and multiple pathways in parallel. Consequently, for many reactions occurring in condensed media (including enzyme-catalyzed reactions) there is no single rate-determining step associated with a unique transition state (TS): in general, any ‘transition-state structure’ derived from experimental kinetics investigations of a complex mechanism is an average corresponding to a virtual TS. Computational simulation is now capable of yielding valuable insight, complementary to experiment, for minima and saddle points on potential-energy surfaces, corresponding to intermediates and TSs on Gibbs-energy surfaces for complex reactions with multiple TSs in parallel or in series. For a reaction with multiple steps in series, the apparent Gibbs energy of activation (corresponding with a virtual TS) is a sum of terms, one for each contributing real TS_{*j*}; the kinetic significance *w_j* of each is given by $\exp(\Delta^\ddagger G_j/RT)/\exp(\Delta^\ddagger G_{\text{app}}/RT)$. An analogous expression applies to the kinetics of reaction steps in parallel, except that each Gibbs energy is preceded by a minus sign, and the contribution *w_i* of each real TS to $\Delta^\ddagger G_{\text{app}}$ is its Boltzmann weighting, and the mole fraction of the lowest-energy reactant conformer must be factored in. Examples of both types of reaction are discussed to illustrate the concept of the virtual TS.

Keywords: computational chemistry; ICPOC-26; isotopes; kinetics; mechanism.

Introduction

The concept of the virtual transition state^{1,2} is probably unfamiliar to most people. Everyone nowadays knows something about virtual reality: by means of a headset, one may experience sights and sounds generated by software, but which do not have external physical existence. Chemists know about virtual orbitals: unoccupied molecular orbitals with no associated electron density and which are therefore unobservable. In common English usage, for something to be described as ‘virtual’ implies a degree of ‘almost’ or ‘nearly’, but ‘not completely’, with respect to something else that is definite and concrete in nature.

It is helpful to start this discussion by briefly recalling the meaning of the terms ‘transition state’ (TS) and ‘transition structure’. The configuration of atoms at the saddle point on a potential-energy surface (PES, Fig. 1a) is a transition structure: it is a molecular entity which has zero forces within its internal degrees of freedom, and which possesses a single imaginary vibrational frequency.¹ The dividing surface passing through the saddle region of a free-energy surface (FES, Fig. 1b) from which there is an equal probability of forming either the reactants or products (of a one-step reaction that has no reaction intermediate) is a TS. It is not identified with a single structure but rather with a set of (micro)states or with an ensemble of configurations each comprising an assembly of atoms possessing a particular geometry and energy.¹ It is important to distinguish these two terms. It is common to see ‘transition state’ used to mean both things, but this practice neglects the very significant difference between (on the one hand) the microscopic scale of a molecular entity and the PES that describes how

Article note: A collection of invited papers based on presentations at the International Conference on Physical Organic Chemistry held on 18–22 Aug 2024 in Beijing, China.

***Corresponding author: Ian H. Williams**, Department of Chemistry, University of Bath, Bath, BA2 7AY, UK, e-mail: i.h.williams@bath.ac.uk. <https://orcid.org/0000-0001-9264-0221>

its potential energy varies as a function of its geometry and (on the other hand) the macroscopic scale of an ensemble of molecular entities and its associated FES.

Many computer codes for electronic-structure calculations generate not only the total electronic energy but also the sum of ‘electronic and thermal free energies’, and many published papers report values of free-energy differences between (say) reactant structures and transition structures. This can be confusing unless care is taken to appreciate what these values may or may not mean. For example, it is not always stated what temperature and standard state have been applied; while this would not affect an activation free energy for an unimolecular rearrangement or dissociation, it could significantly alter a $\Delta^\ddagger G$ value for an associative reaction if (say) a calculation assumes a standard state of 1 atm but the experimental result against which it is wished to compare relates to a standard state of 1 M. Also, it is perhaps not always recognised that the partition-function expressions employed by the computer code probably assume the ideal gas, rigid-rotor, and harmonic-oscillator approximations: this implies that a single molecular entity (say, a transition structure) can serve as an adequate representation of an entire ensemble at the relevant temperature and pressure (or concentration). Thus, it may be unclear how well a computed transition structure models the TS of a reacting system under experimental conditions. More realistic computational simulations may employ molecular dynamics to sample many thermally accessible configurations of such a system, and to propagate multiple reactive trajectories across a FES, most of which lie within a relatively small swathe (coloured pale in Fig. 1b) around a minimum free-energy path (thick black line) between reactants *R* and products *P*. The more extensive the sampling of configurations within relevant regions of the FES, the better the TS is represented by the simulation.

One more term whose meaning is worth clarifying at this stage is ‘transition-state structure’ (or TS structure). Sometimes this expression is applied loosely, as if it is unclear whether it is intended to mean ‘TS’ or ‘transition structure’, but this term does have its own distinct and useful meaning to denote a structure *inferred* from experiment for the TS of a chemical reaction.¹ Experimental determinations of chemical kinetics provide indirect probes of the TS for a reaction. For example, the temperature dependence of an observed rate constant may yield the enthalpy and entropy of activation, but the significance of these values must be interpreted within transition-state theory. Linear free-energy relationships between logarithms of relative rate constants and some measure of structural variation (for example, substituent constants in a Hammett plot or pK_a values in a Brønsted plot), yield slopes whose magnitude and direction are often interpreted as being attributes of the TS, but these are indirect

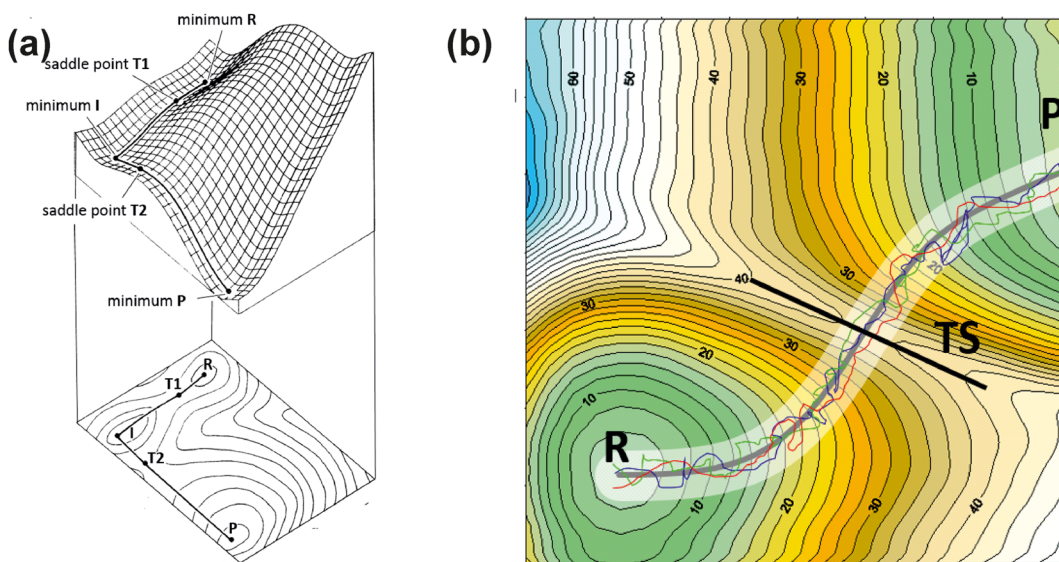


Fig. 1: (a) Upper: 3D representation of a potential-energy surface (PES) with plotted as a function of two coordinates; lower: 2D iso-potential contour map obtained by projection of the PES onto the base plane. (b) 2D free-energy surface obtained as a function of two coordinates. Relative energy contours are coloured from green (low) to blue (high). *R*, *P* and *TS* indicates the regions corresponding to reactants, products and transition state.

inferences. Similarly, kinetic isotope effects (KIEs) are determined by the very subtle influence of one or more extra neutrons in the nucleus of a particular atom within a reacting molecule, without altering the PES, and they may report upon bonding changes occurring between reactants and products. However, the magnitude and direction of an observed KIE must also be interpreted within some framework that provides an indirect link to the presumed TS structure.

Transition states in series and in parallel

Most chemical reactions of interest are not completed in a single elementary step. It may be that one or more intermediates occur along the reaction path that connects reactants and products, in which case there is a TS for each individual consecutive step in the reaction sequence: there are several TSs in series. Or it may be that multiple separate paths connect the same reactants and products in competing reactions, such that there are several TSs in parallel. In either case, TS structures inferred from observed kinetic parameters do not describe any single one of these contributing individual TSs but rather a weighted average of them, which is the virtual transition-state.² If one individual TS tends to be predominant in either case, then its properties and structure will largely determine the inferred properties and structure of the virtual TS, but with a degree of ‘almost’, ‘nearly’, and ‘not completely’. It is of interest to note that the virtual TS is an imaginary species represented as an average of real TSs, in contrast to the picture of a resonance hybrid as being a real structure represented as an average of imaginary structures.²

The response to changes in reaction conditions (for example, temperature, pressure, solvent, or isotopic substitution) of a reacting system involving multiple TSs in series or parallel is a weighted-average response from all the contributing TSs, but it may not be obvious that the response reports on a single ‘pure’ TS or on a virtual TS. One experimental technique for discriminating between these two possibilities in steady-state enzyme-catalysed reactions is based on comparison of observed deuterium and tritium isotope effects on k_{cat}/K_m (where this factor corresponds to the rate constant for the catalysed reaction with respect to free substrate and unbound enzyme in solution),³ and this method has been used extensively by mechanistic enzymologists over many years.⁴ It has been noted that where two reaction pathways lead to the same product, the observed KIE is dominated by the contribution from the TS of lower energy, but for reactions involving multiple steps in series, it is the TS of highest energy that contributes most.⁵ The key point is that observed kinetic parameters do not necessarily have a simple correspondence to a single TS, let alone a single transition structure, and that in these circumstances a TS structure inferred from experimental observations is not a real physical entity.

Reactions in parallel

A trivial example of two reaction pathways in parallel is where achiral reactants lead to an achiral product by means of a pair of enantiomeric TSs. Consider the addition of a single water molecule to formaldehyde (in a gaseous reaction) yielding methanediol, $\text{H}_2\text{O} + \text{CH}_2=\text{O} \rightarrow \text{HOCH}_2\text{OH}$. As it happens, this was the first published example of a transition structure computed by means of ab initio gradient methods,⁶ but the significant point is that the transition structure is chiral (Fig. 2). If observed rate constants for this reaction with (say) H_2O and D_2O were to be compared, the KIE would inevitably be interpreted as arising from a symmetric TS structure (in which the non-transferring hydrogen atom would be coplanar with the heavy atoms and the transferring hydrogen) whereas in fact it would arise from equal contributions of enantiomeric TSs: the inferred structure would be that of the virtual TS.

A less trivial example of parallel TSs for competing reaction pathways comes from consideration of 4,4'-dimethoxybenzhydrylpyridinium cation solvolysis in ethanol. There are four reactant conformers that differ only in the relative orientations of the methoxy substituents, and each is linked directly to a specific transition structure for heterolysis of the scissile C-N bond leading to formation of a benzhydryl cation intermediate that then undergoes nucleophilic attack by ethanol (Scheme 1). It was demonstrated recently that the correct apparent

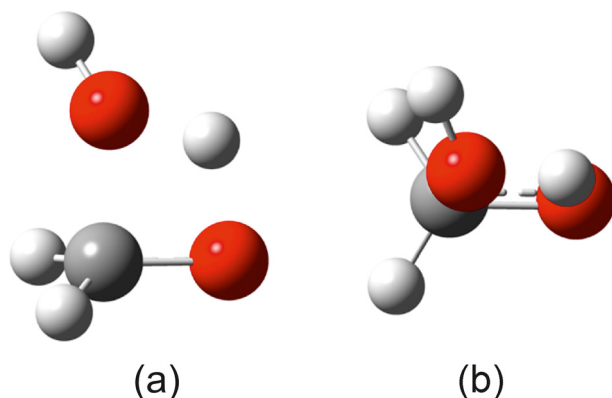
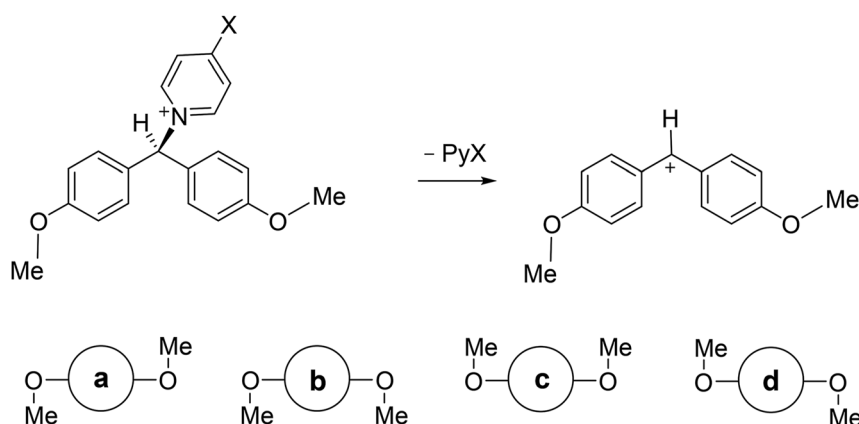


Fig. 2: Computed transition structure (HF/4-31G) for addition of water to formaldehyde: (a) 'side' view, (b) 'top' view.



Scheme 1: Top: heterolysis of one conformer of

4,4'-dimethoxybenzhydrylpyridinium cation. Bottom: cartoon representations for other reactant conformers a, b, c and d to illustrate methoxy-group orientations.

Gibbs energy of activation for N multiple reaction pathways in parallel, arising from a set of rapidly inter-converting reactant conformers (i.e. Curtin-Hammett conditions⁷), may be obtained by eqn (1), which derives the fact that the observed rate coefficient is the sum of the individual rate constants, one for each separate pathway. This equation involves the Gibbs energy $\Delta^\ddagger G_i$ for each individual TS conformer i relative to the reactant-structure conformer of lowest Gibbs energy,⁸ where x_0 is the equilibrium mole fraction of that lowest-energy reactant conformer. The term within the curly brackets is equivalent to the ratio of partition functions for the TS and reactant state (RS), but it is convenient to evaluate it using computed values of Gibbs energies for the relevant structures.

$$\Delta^\ddagger G_{\text{app}}^{\text{parallel}} = -RT \ln \left\{ x_0 \sum_i^N \exp \left[-\Delta^\ddagger G_i / RT \right] \right\} \quad (1)$$

Figure 3 shows Gibbs energies computed⁸ for heterolysis of these cations at the M06-2X/6-311+G(2d,p)/PCM=EtOH level of density functional theory (298 K, 1 M), and all are relative to the energy of conformer **a**; the respective mole fractions are obtained as normalised Boltzmann populations (at 298.15 K): $x_0 = x_a = 0.52$, $x_b = 0.15$, $x_c = 0.17$, $x_d = 0.15$. All four reactant conformers lie within 3 kJ mol^{-1} of each other and are interconverted by internal rotations involving transition structures (dashed black lines) for clockwise directions of rotation. There are separate transition structures for anticlockwise rotations, but their relative energies all lie within the range shown in Fig. 3 ($17.0\text{--}19.5 \text{ kJ mol}^{-1}$), which are very low as compared with the individual activation Gibbs energies

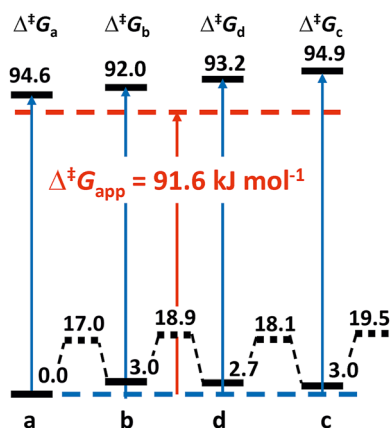


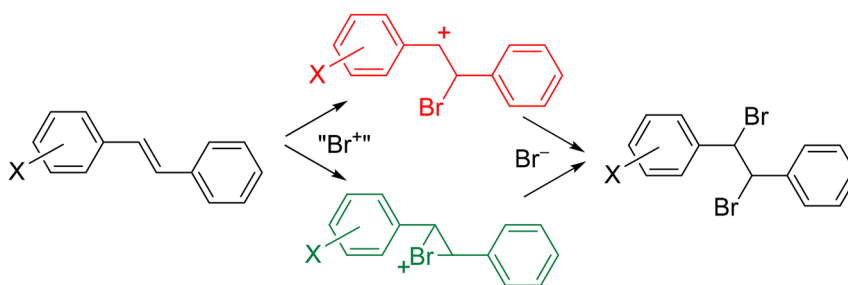
Fig. 3: Computed Gibbs energies [M06-2X/6-311+G(2d,p)/PCM=EtOH] for heterolysis of 4,4'-dimethoxybenzhydrylpyridinium cation (298 K, 1 M), all relative to reactant conformer a. Energies of individual TSs for heterolysis are depicted by vertical blue lines, and for interconversion of reactant conformers are depicted by dashed back lines.

for heterolysis (indicated by vertical blue lines), and the system therefore satisfies Curtin-Hammett conditions. Application of eqn (1) yields an apparent Gibbs energy of activation $\Delta^\ddagger G_{\text{app}}^{\text{parallel}}$ for heterolysis equal to 91.6 kJ mol^{-1} , a value *lower* than any of the individual values of $\Delta^\ddagger G_i$. This is a characteristic feature of reactions occurring by multiple pathways in parallel. The largest share of the total reaction flux between reactants and products proceeds via the transition structure with the lowest Gibbs energy, and the other transition structures contribute smaller shares in proportion to their Boltzmann populations. It is clear that each value of $\Delta^\ddagger G_i$ corresponds to an individual transition structure, which approximately represents the TS for a separate reaction pathway, but to what does the apparent Gibbs energy of activation $\Delta^\ddagger G_{\text{app}}^{\text{parallel}}$ correspond? The answer, of course, is that it corresponds to the virtual TS for the overall reaction: it is a weighted average of all four individual contributing TSs, and it is not a real physical entity. To quote Stein:⁵ ‘For reactions in which more than a single TS is kinetically significant, any experiment designed to probe the structure of the rate-limiting TS will yield information not about a single, real TS, but rather about a “virtual” TS whose structure is a weighted average of structures of the several rate-limiting, real TSs.’

It is well known that a Hammett plot for a reaction of substituted-aryl substrates involving a change in mechanism displays concave-upward behaviour, an example of which is the electrophilic bromination of *trans*-monosubstituted stilbenes in methanol (Scheme 2).⁹ The logarithms of reduced second-order rate constants $\{k_{\text{obs}}\}$ for the most strongly electron-donating substituents correlate with σ^+ giving $\rho = -5.56$ (red points, Fig. 4), while electron-withdrawing substituents yield $\rho = -1.65$ when correlated against σ (green points, Fig. 4). (Note: $\{k_{\text{obs}}\} = k_{\text{obs}}/[k_{\text{obs}}]$, where $[k_{\text{obs}}]$ represents the units of k_{obs} ,¹⁰ in this case $\text{M}^{-1} \text{min}^{-1}$; much common usage and many textbooks incorrectly attempt to construct Hammett correlations using dimensioned rate constants, whereas a logarithm only has strict mathematical meaning for a quantity with dimension = 1.) The solid black curve in Fig. 4 is obtained from the logarithm of the apparent rate constant given by eqn (2). The blue points represent the observed rate constants for $X = m\text{-Me}$ and H : they lie above both the extrapolated red and green dotted lines but are correlated well by the solid black curve, demonstrating that both competing mechanisms contribute to the apparent rate constant, namely parallel pathways via TSs resembling either an open carbocation (strongly electron-donating substituents, Scheme 2) or a cyclic bromonium cation (electron withdrawing substituents, Scheme 2). The virtual TS corresponding to this region of the Hammett plot is an average of these two real TSs.

$$k_{\text{app}} = k_{\text{red}} + k_{\text{green}} = \text{antilog}(-5.56\sigma^+ + 0.70) + \text{antilog}(-1.65\sigma^+ + 1.29) \quad (2)$$

With reference to the earlier discussion of trajectories across a FES (Fig. 1), each of the open carbocation and cyclic bromonium cation pathways (Scheme 2) corresponds to a distinct swathe of microscopic trajectories around a particular minimum free-energy path. The overall FES contains two separate saddle regions separated by a local maximum, and there is a unique FES for each substituent group X with different weightings for the pair of real TSs



Scheme 2: Alternative mechanisms for electrophilic bromination of *trans*-monosubstituted stilbenes. Strongly electron-donating substituents favour the upper path via the open carbocation (red); electron withdrawing substituents favour the lower path via the cyclic bromonium cation (green).

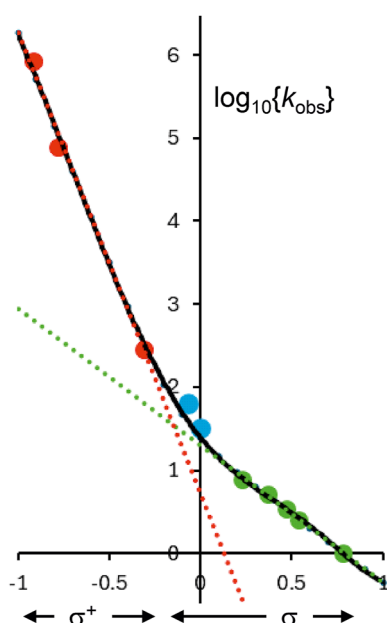


Fig. 4: Hammett plot for electrophilic bromination of stilbenes. Red points denote strongly electron substituents (vs. σ^+), green points denote electron-withdrawing substituents (vs. σ), and blue points denote X = *m*-Me and H; the solid black curve is represented by eqn (2).

in parallel. The virtual TS should not be confused with the averaging of microscopic trajectories for a single reaction pathway.

Reactions in series

A curious (although perhaps also trivial) example of a stepwise reaction involving multiple TSs in series arises from a computational study of the identity reaction $\text{H}_2\text{O} + {}^t\text{BuOH}_2^+ \rightarrow {}^t\text{H}_2\text{O} + \text{OH}_2$ at the HF and B3LYP/6-31G*/PCM=water levels of electronic structure theory, which occurs as a sequence of individual methyl-group rotations superimposed on an overall $\text{S}_{\text{N}}2$ Walden inversion;¹¹ in practice this reaction would follow pseudo first-order kinetics. As expected, each TS is very carbocationic in character, with a “ Bu^+ ” moiety sandwiched between a pair of water molecules. It may come as a surprise to recognise that, if this displacement reaction were to occur solely by Walden inversion coupled with asymmetric motion of the nucleophile and nucleofuge, the product would have its methyl groups eclipsing with the new C–O bond. Methyl-group rotation is therefore an essential component necessary to attain an identical staggered product; the process could occur in a single-step concerted reaction, but with the particular computational method employed in this study it is predicted to involve a series of three separate transition structures, as shown in Fig. 5. Inspection of the transition vector for each transition structure reveals a predominant rotation of just one methyl group at a time about the C–C bond connecting it to the

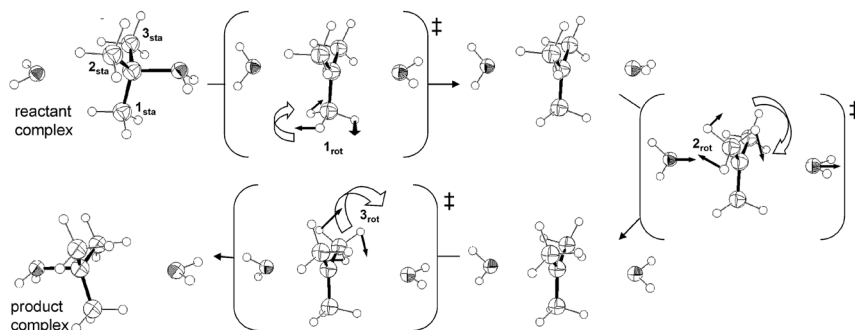


Fig. 5: HF/6-31G*/PCM=water computed transition structures for the identity reaction $\text{H}_2\text{O} + {}^t\text{BuOH}_2^+ \rightarrow {}^t\text{H}_2\text{OBu}^t + \text{OH}_2$. (N.B. all optimised structures and the topography of the minimum-energy reaction path are qualitatively the same at the B3LYP/6-31G*/PCM=water level of computational theory.)

carbocationic centre. The product complex possesses three staggered methyl groups (1_{sta} , 2_{sta} and 3_{sta}) like the reactant complex.

It should be noted that the use of a more accurate and reliable computational method than was available in 2001¹¹ might (or might not) yield a different picture – for example, a single transition structure with synchronous methyl-group rotations – but that is not the point of the present discussion, which is rather to illustrate the possibility that an experimentally derived transition-state structure may be a virtual TS.

The situation is actually more complicated than shown in Fig. 5 because each of the three steps can occur by either of two parallel paths, according to the direction of methyl-group rotation: details may be found in the original paper.¹¹ For the present purpose it is sufficient to note that the transition structures for the first and third steps, and the two intermediates, are enantiomerically related, and the transition structure for the second step is also chiral. At the B3LYP/6-31G*/PCM=water level of calculation, the Pauling bond order of each C...O partial bond in the central transition structure is approximately 0.19, indicating a substantial degree of carbocationic character, but the transition vector has an imaginary frequency of $195i \text{ cm}^{-1}$, which is further evidence that the ${}^t\text{Bu}$ moiety does not lie in an energy minimum. The total electronic energy of the equivalent intermediates is 58 kJ mol^{-1} higher than the reactant complex, with barriers of 6.8 and 11.1 kJ mol^{-1} to the equivalent first/third and second transition structures, respectively: this implies that the intermediates would be very short-lived and thence that the steady-state approximation may be safely applied.

$$\Delta^\ddagger G_{\text{app}}^{\text{series}} = RT \ln \left\{ \sum_j^M \exp \left[\Delta^\ddagger G_j / RT \right] \right\} \quad (3)$$

The apparent Gibbs energy of activation for a steady-state system of M reaction steps in series is given by eqn (3), where $\Delta^\ddagger G_j$ is the Gibbs energy of each sequential TS j relative to a common RS; this equation derives the fact that the reciprocal of the observed rate coefficient is the sum of the reciprocals of the individual rate constants, each relative to the same RS. Comparison with the similar-looking eqn (1) shows two important differences. First, since there is only one RS, its mole fraction is unity, and therefore x_0 does not appear in eqn (3). Second, the latter equation has plus signs where eqn (1) has minus signs. The B3LYP/6-31G*/PCM=water values of $\Delta^\ddagger E_j$ for the three TSs in Fig. 5 are 64.8 , 69.1 and 64.8 kJ mol^{-1} , respectively; assuming (for the purposes of illustration) that relative Gibbs energies may be approximated by relative total electronic energies, then insertion of these values into eqn (3) leads to an apparent activation energy of 69.9 kJ mol^{-1} , which is *higher* than any of the individual values of $\Delta^\ddagger E_j$. This is a characteristic feature of reactions occurring by multiple steps in series: it is harder to cross the entire sequence of TSs in series than to surmount any single one. The extent to which each TS contributes to the overall apparent activation energy is given by eqn (4), where w_j is a weighting factor, otherwise known as the kinetic significance of TS j .

$$w_j = \exp[\Delta^\ddagger G_j/RT] / \left\{ \sum_j^M \exp[\Delta^\ddagger G_j/RT] \right\} \quad (4)$$

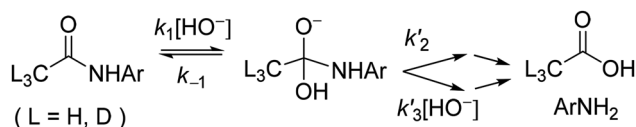
Using the three values of $\Delta^\ddagger E_j$ given above (and approximating $\Delta^\ddagger G$ by $\Delta^\ddagger E$ in eqn (4)), the respective weighting factors for the three TSs in Fig. 5 are 0.13, 0.74 and 0.13, which shows that the TS of most kinetic significance is that with the highest energy. These weighting factors are not mole fractions deriving from Boltzmann populations; perhaps they may be called anti-Boltzmann weightings. As with the example of parallel TSs considered above, the question to be asked is: to what does the apparent Gibbs energy of activation for a multi-step reaction with TSs in series correspond? And, again, the answer is a virtual TS. In the present example this may be considered as relating to nucleophilic displacement with Walden inversion, but with undefined methyl-group conformations; it is amusing to note that the virtual TS may be imagined as conforming to what an S_N2 -like mechanism is expected to 'look' like despite each of the actual transition structures telling part of a somewhat different story.

Complex reactions in series and parallel

There are many complex reaction systems, including both enzyme-catalysed and nonenzymic examples, in which several different processes may simultaneously contribute to limiting the reaction rate. Consequently, any observed property (e.g. an isotope effect, or the slope of a linear free-energy relationship) that reports on TS-behaviour may be a complicated average of the effects on the elementary steps, reflecting a virtual TS. An early example, involving multiple steps in series and in parallel, considered variations in observed β -deuterium KIEs for hydrolysis of *p*-nitroacetanilide in basic solution.¹² Not only did the observed KIE for *p*-NO₂C₆H₄NHCOCH₃ versus NO₂C₆H₄NHCOCD₃ change from 0.967 ± 0.011 in the least-basic solution, rise to about 0.98 with increasing hydroxide-ion concentration, and fall to 0.933 ± 0.020 in the most-basic solution, but also an apparently anomalous temperature dependence was found which would have required implausible values for the Arrhenius preexponential factor A_H/A_D and the isotopic activation energy difference ΔE_a if a single TS were responsible. The more reasonable explanation proposed was a shift in limitation of the rate away from the k_1 TS (for formation of an anionic quasi-tetrahedral intermediate, Scheme 3) toward the k_3 TS (for decomposition of a dianionic intermediate, Scheme 3), as $[HO^-]$ increased or as the temperature was raised. At low $[HO^-]$ decomposition of the adduct initially gives CL₃CO₂H + NO₂C₆H₄NH[−] (where L = H or D), whereas at high $[HO^-]$ there is competing decomposition of the deprotonated adduct (initially to CL₃CO₂[−] + NO₂C₆H₄NH[−]). The reciprocal of the phenomenological rate constant k_0 (corrected from the observed rate constant for ionisation of the anilide substrate¹²) is given by eqn (5), where $k_2 = k'_2(k_1/k_{-1})$ and $k_3 = k'_3(k_1/k_{-1})$ are rate constants with respect to neutral substrate, and the β -deuterium KIE, $k_0(CH_3)/k_0(CD_3)$, is given by eqn (6) with weighting factors as shown in eqn (7).

$$\frac{1}{k_0} = \frac{1}{k_1[HO^-]} + \frac{1}{k_2[HO^-] + k_3[HO^-]^2} \quad (5)$$

$$k_0(CH_3)/k_0(CD_3) = w_1({}^Hk_1/{}^Dk_1) + \left\{ \left[w_2({}^Hk_2/{}^Dk_2)^{-1} \right] + \left[w_3({}^Hk_3/{}^Dk_3)^{-1} \right] \right\}^{-1} \quad (6)$$



Scheme 3: Stepwise mechanism for anilide hydrolysis in basic solution.

$$w_1 = \frac{{}^Hk_0}{{}^Hk_1[\text{HO}^-]} \quad w_2 = \frac{{}^Hk_0}{{}^Hk_2[\text{HO}^-]} \quad w_3 = \frac{{}^Hk_0}{{}^Hk_3[\text{HO}^-]^2} \quad (7)$$

Conclusion

Since its inception in 1978,² and early applications from some of Schowen's co-workers [e.g. 5, 12], the concept of the virtual TS has been largely overlooked. The reason for this apparent neglect is more likely to be that there remain significant practical difficulties to identify each contributing real TS and to derive its kinetic significance than that the notion itself is of no value. This author considers that it is now potentially of more use than previously owing to modern developments in methods for computational simulation of chemical reaction mechanisms which are capable of locating and characterising TSs for reactions in solution or catalysed by enzymes. It is helpful to be reminded that the entity inferred from experiment and regarded as 'the' TS is often an average of several contributing TSs which may be studied by simulation. All attempts to bridge the gap between theory and experiment must take note of this fact and should avoid unhelpful over-simplification. It may be better for comparisons between theory and experiment to be made at the level of the virtual TS.

Acknowledgments: The organisers of ICPOC26 are thanked for the opportunity to present a short preliminary version of this work in August 2024.

Research ethics: Not applicable.

Informed consent: Not applicable.

Author contributions: The author has accepted responsibility for the entire content of this manuscript and approved its submission.

Use of Large Language Models, AI and Machine Learning Tools: None declared.

Conflict of interest: The author states no conflict of interest.

Research funding: None declared.

Data availability: Not applicable.

References

1. Tuñón, I.; Williams, I. H. The Transition State and Cognate Concepts. *Adv. Phys. Org. Chem.* **2019**, *53*, 29–68. <https://doi.org/10.1016/bs.apoc.2019.09.001>.
2. Schowen, R. L. Catalytic Power and Transition-State Stabilization. In *Transition States of Biochemical Processes*; Gandour, R. D.; Schowen, R. L., Eds.; Plenum Press: New York, 1978; pp 77–114.
3. Northrop, D. B. Steady-State Analysis of Kinetic Isotope-Effects in Enzymic Reactions. *Biochemistry* **1975**, *14*, 2644–2651. <https://doi.org/10.1021/bi00683a013>.
4. Cleland, W. W. The Use of Isotope Effects in the Detailed Analysis of Catalytic Mechanisms of Enzymes. *Bioorg. Chem.* **1987**, *15*, 283–302. [https://doi.org/10.1016/0045-2068\(87\)90026-5](https://doi.org/10.1016/0045-2068(87)90026-5).
5. Stein, R. L. Analysis of Kinetic Isotope Effects on Complex Reactions Utilizing the Concept of the Virtual Transition State. *J. Org. Chem.* **1981**, *46*, 3328–3330. <https://doi.org/10.1021/jo00329a036>.
6. Williams, I. H.; Spangler, D.; Femec, D. A.; Maggiora, G. M.; Schowen, R. L. Theoretical Models for Mechanism and Catalysis of Carbonyl Addition. *J. Am. Chem. Soc.* **1980**, *102*, 6619–6621. <https://doi.org/10.1021/ja00541a068>.
7. Seeman, J. I. Effect of Conformational Change on Reactivity in Organic Chemistry. Evaluations, Applications, and Extensions of Curtin-Hammett/Winstein-Holness Kinetics. *Chem. Rev.* **1983**, *83*, 83–134. <https://doi.org/10.1021/cr00054a001>.
8. Williams, I. H. Gibbs Energies of Activation for Reacting Systems with Multiple Reactant-State and Transition-State Conformations. *J. Phys. Org. Chem.* **2022**, e4312. <https://doi.org/10.1002/poc.4312>.
9. Ruasse, M.-F.; Dubois, J.-E. Electrophilic Bromination of Aromatic Conjugated Olefins. I. Evaluation of a Competitive Path Mechanism in Bromination of Trans-monosubstituted Stilbenes. *J. Org. Chem.* **1972**, *37*, 1770–1778. <https://doi.org/10.1021/jo00976a023>.

10. Perrin, C. L.; Agranat, I.; Bagno, A.; Braslavsky, S. E.; Fernandes, P. A.; Gal, J.-F.; Lloyd-Jones, G. C.; Mayr, H.; Murdoch, J. R.; Nudelman, N. S.; Radom, L.; Rappoport, Z.; Ruasse, M.-F.; Siehl, H.-U.; Takeuchi, Y.; T. T.; Tidwell, T. T.; Uggerud, E.; Williams, I. H. Glossary of Terms Used in Physical Organic Chemistry (IUPAC Recommendations 2021). *Pure Appl. Chem.* **2022**, *94*, 353–534. <https://10.1515/pac-2018-1010>.
11. Ruggiero, G. D.; Williams, I. H. Computational Investigation of the Effect of α -Alkylation on S_N2 Reactivity: Acid-Catalyzed Hydrolysis of Alcohols. *J. Chem. Soc., Perkin Trans.* **2001**, *2*, 448–458. <https://doi.org/10.1039/b100214g>.
12. Stein, R. L.; Fujihara, H.; Quinn, D. M.; Fischer, G.; Küllertz, G.; Barth, A.; Schowen, R. L. Transition-State Structural Features for Anilide Hydrolysis from β -Deuterium Isotope Effects. *J. Am. Chem. Soc.* **1984**, *106*, 1457–1461. <https://doi.org/10.1021/ja00317a045>.